Samples of the initial products after mixing the reactants and the end products obtained after complete oxidation are studied by the aid of Mössbauer spectroscopy, X-ray diffraction and transmission electron microscopy.

A mixture of x mol ℓ^{-1} $FeSO_4$ and y mol ℓ^{-1} of NaOH was found to give rise to three main types of initial reaction. These regions were found to depend upon the initial ratio of reagents, R, defined as

$$R = \{[FeSO_4]/[NaOH]\}_{initial} = \{[Fe^{2+}]/[OH^-]\}_{initial} = \{[SO_4^{2-}]/[OH^-]\}_{initial} = x/y$$

The initial products depend on whether one is dealing with a stoichiometric condition (R = 0.5), excess OH^- (basic) or excess of Fe^{2+} (acidic). Thus the formal reactions for each condition can be considered:

Stoichiometric condition, i.e. $R = 0.5 \Leftrightarrow y = 2x$. This corresponds to the stoichiometric precipitation of $Fe(OH)_2$ from the reactants. The equation can be written as follows:

$$FeSO_4 + 2NaOH \rightarrow Fe(OH)_2 + Na_2SO_4 \qquad \text{[III.14]}$$

Basic conditions, i.e. $R < 0.5 \Leftrightarrow y = 2x$. Under this condition all initial Fe^{2+} ions are consumed to precipitate $Fe(OH)_2$ and some OH^- ions are left in the solution. The initial reaction is as follows:

$$xFeSO_4 + yNaOH \rightarrow xFe(OH)_2 + xNa_2SO_4 + (y-2x)Na^+ + (y-2x)OH^- \qquad \text{[III.15]}$$

Experiments performed in this region of R are termed reactions in *basic medium*, as the OH^- ions are always in excess. If X_b is the concentration ratio of the excess OH^- ions in the solution to that of the precipitated $Fe(OH)_2$, then,

$$X_b = \{[OH^-]_{sol}/[Fe(OH)_2\}_{initial} = (y-2x)/x = 1/R_b - 2 \qquad \text{[III.16]}$$

where the index 'b' means basic.

Acidic conditions, i.e. R > 0.5 ⇔ y = 2x. Contrary to the basic condition, all initial OH^- ions are consumed to precipitate $Fe(OH)_2$ leaving some excess Fe^{2+} ions in the solution. The initial reaction is as follows:

$$xFeSO_4 + yNaOH \rightarrow y/2Fe(OH)_2 + y/2Na_2SO_4 + (x-y/2)Fe^{2+} + (x-y/2)SO_4^{2-} \qquad \text{[III.17]}$$

Similarly, we can denote the initial concentration ratio of the excess Fe^{2+} ions in the solution to that of the precipitated $Fe(OH)_2$ by X_a, to obtain,

$$X_a = \{[Fe^{2+}]_{sol}/[Fe(OH)_2]\}_{initial} = (x-y/2)/(y/2) = 2R_a - 1 \qquad \text{[III.18]}$$

where the index 'a' means acidic or neutral. Although reactions in this range of R more often start at a slightly basic value of pH, they always end up in the acidic range. They will thus be characterized as reactions in the *acidic medium.*

Evidently, from equations [III.16] and [III.18] above, $X_a = X_b = 0$ when $R_a = R_b = 0.5$, i.e. at the transition value of R between acidic and basic media, when stoichiometry is fulfilled by $Fe(OH)_2$.

The establishment of the various mechanisms of oxidation is achieved by investigating the influence of the factor R on the initial and end products of oxidation. The main conclusion drawn from earlier studies was the identification of a characteristic value of R = 0.625 (labeled point E) above which the initial product ceased to be the regular ferrous hydroxide but a basic sulphate $xFe(OH)_2$, $yFeSO_4$ within which a crystallized phase $4Fe(OH)_2$; $FeSO_4$; nH_2O named sulphated ferrous

hydroxide (SFH) has been identified by the aid of Mössbauer and X-ray diffraction analyses. This characteristic point E is obtained as follows:

$$X_a = 2R_a - 1 = 1/4 \leftrightarrow R_a = 0.625, \qquad \text{[III.19]}$$

i.e. when one mole of $FeSO_4$ from the Fe^{2+} and SO_4^{2-} ions of the solution matches four moles of $Fe(OH)_2$ precipitated.

Experiments were carried out so as to maintain 0.1 M $Fe(OH)_2$; thus for $R < 0.5$ the initial concentration of $FeSO_4$, x, is fixed at 0.1 M and for $R > 0.5$ the initial concentration of NaOH, y, is fixed at 0.2 M.

III.F.1 The E_h/time and pH/time Experimental Curves

The various E_h and pH curves with respect to time, as obtained from the recorder, are presented in Figure III.33. The E_h curves are separated by 0.5 V and the pH curves by 2.5 to aid in viewing the graphs. For convenience of presentation, increasing values of E_h are drawn downward. The numbered points correspond to the various equilibrium points (see text to see details). Nevertheless, each point of inflexion characterized by a time t, corresponds to a change of phase, of which one of the products is completely disappearing. This technique is useful to determine the number of stages involved for each value of R. All experiments start at point t_o and terminate at point t_f. In the situation where two inflexion points appear, i.e. for $R > 0.5$, time t_g is used to define the end of the first stage of oxidation. Each experiment is left to continue until the final equilibrium is reached between the final products and the solution.

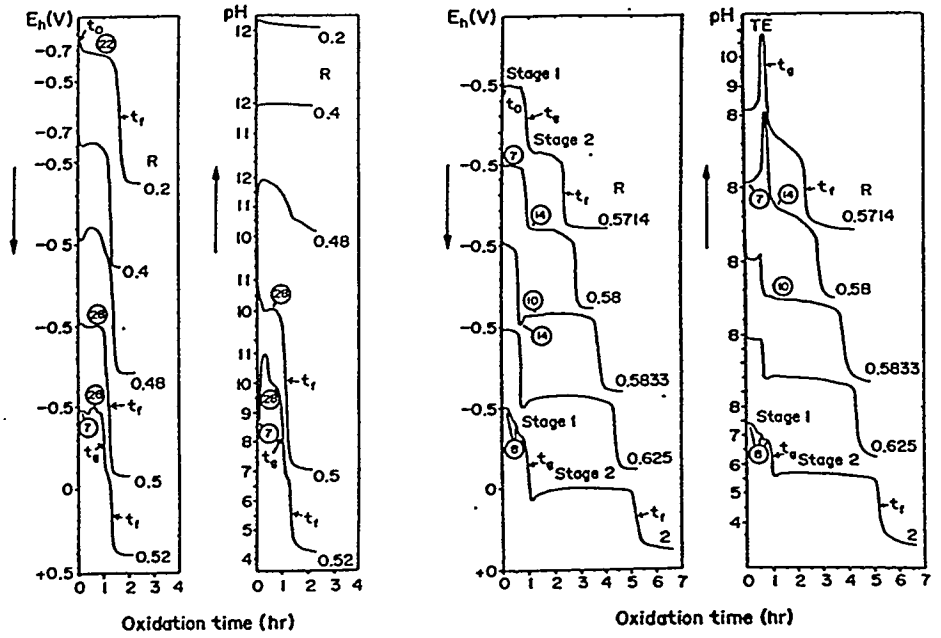

Figure III.33. **Recorded experimental curves of E_h and pH with respect to oxidation time at 25°C for various values of R = $[FeSO_4]/[OH^-]$. E_h is with respect to hydrogen standard and increasing value direction is downward. $R \leq 0.44$: domain of formation of geothite and α'-FeOOH particles. $0.48 \leq R \leq 0.5625$: domain of formation of magnetite. $0.565 \leq R \leq 0.58$: domain of formation of geothite from Green Rust 2 (GR2). $R \geq 0.5833$: domain of formation of lepidocrocite (and geothite). t_0: beginning of all reactions; t_f: end of all reactions. t_g: end of all reactions for the first stage for R > 0.5. The circled numbers correspond to equilibria between the following products and they are discussed fully in a separate publication (III.76): ferrous hydroxide and Green Rust 2 (GR2); (III.75): the basic sulphates (1-β)$Fe(OH)_2$, $\beta FeSO_4$ and GR2; (III.2): GR2 and γ-FeOOH; (III.76): GR2 and active α'-FeOOH; (III.26): ferrous hydroxide and α-FeOOH; (III.77): ferrous hydroxide and hydrated magnetite (from reference III.78).**

For R < 0.5 only one stage can be observed and the oxidation process ends up in the *basic medium*.

For R > 0.5, at least two different stages can be observed. This is the first indication of the existence of the transient compound, Green Rust 2 (GR2). The transformations can also globally be presented as follows:

$$\textit{Initial product(s)} \xrightarrow{\textit{stage 1}} GR2 \xrightarrow{\textit{stage 2}} \textit{End products}$$

and the process of oxidation ends up in the *acidic medium*.

However, each stage of the transformations described above can involve a series of consecutive reactions in which one product is fast disappearing and can therefore not be observed on the E_h and pH curves. One thing is certain, no end product is formed simultaneously with GR2 in the region of its existence. One can notice the sharp rise of the pH for stage 1, for $0.5 < R < 0.5833$ (7/12), indicating probably a partial dissolution of ferrous hydroxide within this region. This ceases completely at $R = 0.625$.

The idea of defining acidic and basic media with respect to R can be more clearly seen by plotting the E_h and pH at the start of the reaction (point t_0) against R. The transition value of $R = 0.5$ which separates the two media is marked as B in Figure III.34. The same phenomenon is also observed during oxidation in chloride media (III.74). The five other characteristic values of R marked A_1, A_2, C, D and E, correspond to the values of 0.333 (1.3), 0.4, 0.571 (4/7), 0.583 (7/12) and 0.625 (5/8) respectively. They will be more fully discussed later. Meanwhile, one can see that points B, D and E are actually trigger values of R which indicates different mechanisms of transformations.

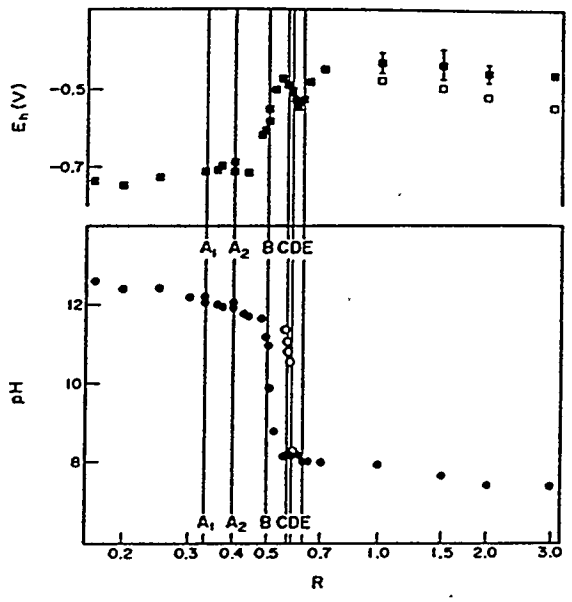

Figure III.34. The electrode potential (E_h) and pH of the reaction at 25°C for different values of R = [$FeSO_4$]/[OH^-]. E_h is with respect to hydrogen standard. Closed square: E_h at the start of the reaction; closed circle: pH at the start of the reaction; open square: minimum E_h attained; open circle: maximum pH attained. The lettered lines correspond to the positions of the characteristic values of R which are respectively from A_1 to E: 0.333 (1/3), 0.4, 0.5 (1/2), 0.571 (4/7), 0.583 (7/12) and 0.625 (5/8) (from reference III.78).

Another way of viewing the characteristic values is to plot the oxidation times, t_e, for various R values as shown in Figure III.35. Figure III.35a shows the overall time for complete oxidation for all R values. Since in the acidic region (R > 0.5) there are two stages in this region and are plotted for two times: $t_e = t_g$ (i.e., the end of the first stage and $t_e = t_f$ for the second stage) (Figure III.35b). In the basic region t_f increases with basicity, indicating that OH^- in solution plays a role in the formation of the final product.

The pH curves (Figure III.33) also show that the *acidic medium* is more properly defined by splitting it into three regions, i.e. for R belonging to [0.5, 0.5833],

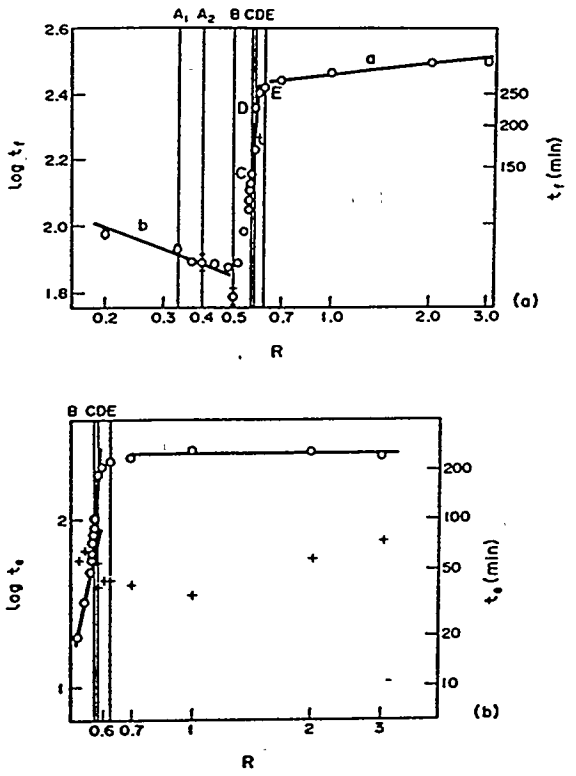

Figure III.35. Overall oxidation time t_e with respect to the initial $[FeSO_4]/[OH^-]$ ratio (R) on a log-log scale. (a) The overall time for complete oxidation (t_f). (b) The time of complete oxidation for each stage for R > 0.5. Crosses are for the first stage ($t_e = t_g$) and circles for the second stage ($t_e = t_f - t_g$). Letters A to E indicates the defined characteristic values of R (from reference III.78).

[0.5833, 0.625] and [0.625, ∞]; or using the notations that define the characteristic values, BD, DE and E∞ respectively. The separation is also easily noticed in Figure III.35. In Figure III.35, the basic medium (line b) is separated from the *steady acidic medium* (E∞) (line a) by a *transition acidic medium* (BD) (line t) and a *quasi-steady acidic medium* (DE) which cannot be described by a line. All newly defined regions still belong to the acidic domain, but with an overall oxidation time in the transition acidic region, very sensitive to R and characterized by a high slope. It is in this transition acidic region, BD, that the previously noted sharp rise in pH for stage 1 of Figure III.33 is observed, as presented in Figure III.32 by the open circles. In the *steady acidic medium* (E∞), t_f is less sensitive to R than in lines b and t. The second

stage (Figure III.33) is almost insensitive to R and we can conclude that it is the first stage that governs the behavior observed in Figure III.33. Within the *transition acidic medium*, it is clearly seen in Figure III.33, that all points for the second stage do not lie on this same line as can also be observed in Figure III.33.

III.F.2. Qualitative Analysis of the End Products

X-ray analysis gives valuable qualitative information about the nature of the products. After the end of each oxidation, the product is rinsed, filtered and dried at room temperature before any physical study is performed. The X-ray diffraction patterns of some of the products are displayed in Figure III.36. The patterns show

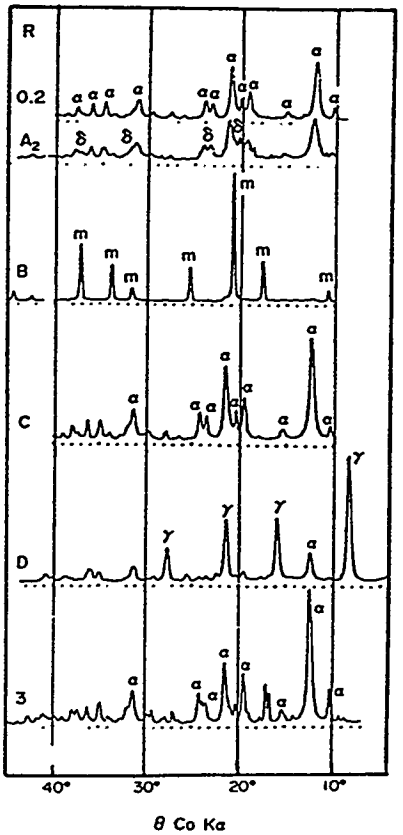

Figure III.36. **X-ray diffraction patterns of the end products of oxidation at 25°C for different values of R = $[FeSO_4]/[OH^-]$. For the letters A_2 to D, the values of R are 0.4, 0.5, 0.571, 0.583 respectively. The diffraction lines that correspond to the different products (from ASTM are indicated. α = geothite; γ = lepidocrocite; m = magnetite (from reference III.78).**

that magnetite, geothite and lepidocrocite are predominant at the characteristic points B, C and D, respectively; of these three end products, only geothite is predominant at low and high values of R. The diffraction lines of α-FeOOH for R = 0.4 are broadened due to the presence of small particles of 'α-FeOOH'.

Some of the samples, especially those obtained from the characteristic values, were investigated using transmission electron microscopy. The pictures also give an idea about the texture of the samples. One notices a cluster of small particles with irregular shape and size into a spongy mass for the samples from points A_1 and A_2. The particles from point A_1 are more or less threadlike and the types of particles observed at point A_2 are similar to those observed and described as cubic crystals by Giessen (III.2). The relatively larger particles of α-FeOOH are seen at R = 0.2 and R = 3. The needle-like particles of γ-FeOOH and the magnetic particles of magnetite could be seen for samples from points D and B, respectively.

Mössbauer spectra were also utilized to identify the products from the oxidation of iron(II) (Figure III.37). The first series ($0.2 \leq R \leq 0.44$) consists mainly of the sextet of geothite (G) with a central doublet (P); the intensity of P increases with R up to the characteristic values A_1 and A_2 after which it diminishes (A_1 and A_2 correspond to the final R at which P is maximum). The second series ($0.48 \leq R \leq 0.563$) consists of a pair of sextets (M1 and M2) of magnetite which is the majority, G which drastically drops to its minimum at point B, and a small amount of P. The third series ($0.565 \leq R \leq 0.58$) has the spectra of products around trigger point C and are essentially identical to G.

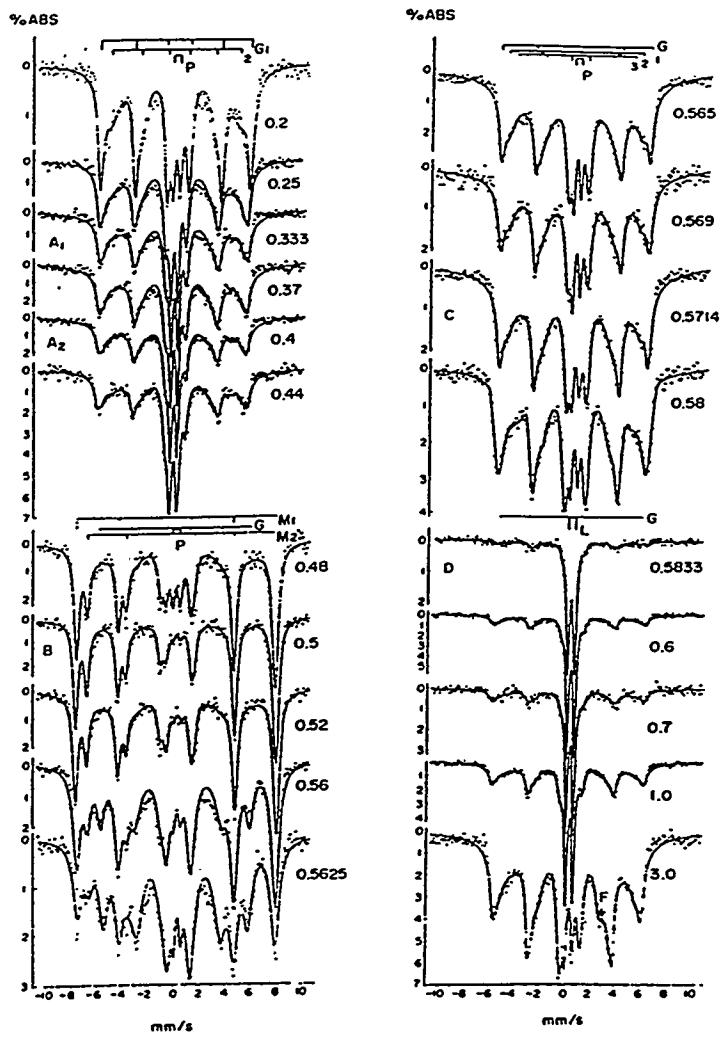

Figure III.37. Mössbauer spectra run at room temperature of the end oxidation products at 25°C for different values of R = $[FeSO_4]/[OH^-]$. R for each spectrum is given at the right-hand side and the characteristic points at the left hand side. G = geothite; P = paramagnetic component; M = magnetite; L = lepidocrocite (from reference III.78).

The final series ($R \geq 0.583$) has a spectrum that, at the start of the series, is mainly L, which suddenly appears at point D at its maximum. The calculated abundances of each phase are given in Table III.5 and are plotted in Figure III.38.

Table III.5

Overall Oxidation Times (in Minutes)* of the Initial Products up to the End Products and the Composition of the End Products of Oxidation at Various Values of R (M = magnetite; G = geothite; P = paramagnetic component; L = lepidocrocite) (from reference III.78)

		Stage 1		Stage 2	Relative Abundance (%)			
	R	t_g	t_f	$t_f - t_g$	M	G	P	L
	0.2		94.5		0	89.3	10.7	0
			(3.6)					
A_1	0.333		84.9		0	79.6	20.4	0
			(2.1)					
	0.37		77.4		0	81.7	18.3	0
A_2	0.4		76.8		0	76.1	23.9	0
			(6.2)					
	0.44		75.9		0	72.3	19.7	0
	0.48		74.8		73.8	17.9	8.3	0
B	0.5		60.9		89.7	7.2	3.1	0
			(5.4)					
	0.52	56.6	76.5	19.9	84.0	12.1	3.9	0
	0.54	64.2	95.7	31.5				
	0.56	65.7	114.8	49.1	61.5	33.5	5.0	0
	0.5625	59.4	119.6	60.2	34.3	60.2	5.5	0
	0.564	54.6	126.0	71.4				
	0.565	52.8	110.3	57.5	0	93.4	6.6	6
	0.569	51.0	132.0	81.0	0	93.2	6.8	0
C	0.5714	51.7	141.8	90.1	0	92.6	7.4	0
	0.58	54.2	169.0	114.8	0	93.7	6.3	0
D	0.5833	38.4	227.4	189.0	0	25.1	0	74.9
	0.6	42.6	251.0	208.4				
E	0.625	42.0	261.0	219.0				
	0.7	39.7	276.2	236.5	0	49.8	0	50.2
	1.0	35.3	291.0	255.7	0	68.4	0	31.6
	2.0	58.7	310.1	251.4				
	3.0	75.0	311.6	236.6	0	92.3	0	7.7

*The given standard deviations are over two to four different experiments.

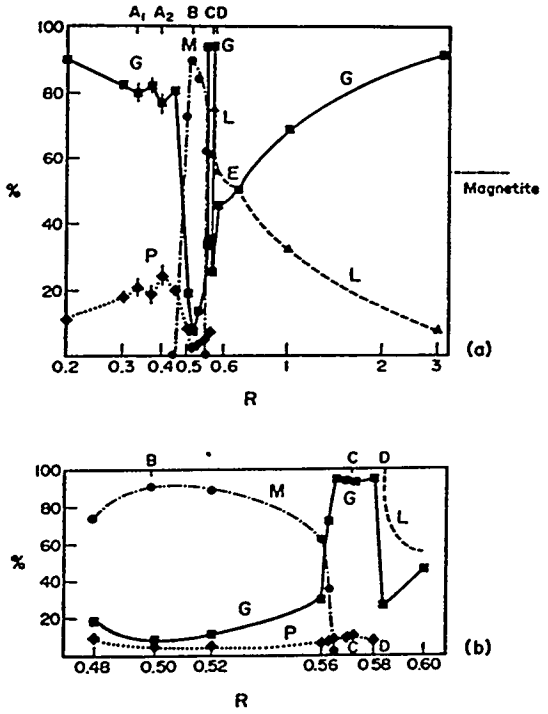

Figure III.38. Plot of the relative abundances of the different end products with respect to R = [$FeSO_4$/[OH^-]: (a) including all the defined characteristic values of R; (b) enlarged portion including the characteristic points B, C and D. M = magnetite (Fe_3O_4); G = geothite (α-FeOOH); L = lepidocrocite (γ-FeOOH); P = paramagnetic component (from reference III.78).

The following summary of the results for the slow oxidation at room temperature is quoted from reference (III.78):

Basic medium (R < 0.5). The oxidation of ferrous hydroxide (FH) is governed essentially by the excess OH^- ions. We can assume that the mechanism of oxidation is as follows:

$$Fe(OH)_2 + X_b\ OH^- = (1-X_b)Fe(OH)_2, X_b FeO_m(OH)_{3-2m} + mX_b\ H_2O + X_b\ e^- \quad \text{[III.20]}$$

where X_b (from equation III.16) measures the extent of oxidation of FH and $0 < m < 1$ is such that m/2 is the degree of deprotonation. Since equation [III.20] involves the consumption of the OH^- ions, the solution will always remain basic by the supply of OH^- from the cathodic reaction:

$$1/4 X_b O_2 + (1/2) X_b H_2O + X_b e^- = X_b OH^- \quad \text{[III.21]}$$

and by adding equation [III.20] and [III.21], we obtain the overall reaction:

$$Fe(OH)_2 + (1/4) X_b O_2 + (1/2 - m) X_b H_2O \rightarrow (1 - X_b) Fe(OH)_2, X_b FeO_m(OH)_{3-2m}. \quad \text{[III.22]}$$

For the specific values of R corresponding to points A_1 and A_2, one has:

for point A_1, $R = 1/3 \Leftrightarrow X_b = 1$

for point A_2, $R = 5/12 \Leftrightarrow X_b = 0.4$.

This will lead to the formation of two basic intermediate compounds:

$FeO_m(OH)_{3-2m}$ at point A_1

and

$Fe(OH)_2, FeO_m(OH)_{3-2m}$ at point A_2

The oxidation processes take place only by deprotonation. Therefore the Fe/O ratio at the beginning of the reactions will be conserved in the intermediate. This means that the values of R at these characteristic points correspond to the Fe/O ratio in the intermediate compounds formed during the oxidation. If we thus compare the Fe/O ratio in the intermediate compounds with the values of R at points A_1 and A_2, we obtain the probable chemical compositions of the intermediate compounds:

for point A_1, $R = 1/3 \Leftrightarrow Fe(OH)_3$

and

for point A_2, $R = 5/12 \Leftrightarrow 3Fe(OH)_2, 2Fe(OH)_3$.

Point A_1. The assumption that point A_1 is a characteristic point is based on the slight increase in the composition of the paramagnetic component as obtained from

Mössbauer analysis and the texture of the particles as seen from electron micrographs; this assumption will need to be confirmed by other experimental techniques. Actually, Baudisch and Mayer (III.79) in 1920 used the same concept to explain the formation of $Fe(OH)_3$ from ferrous hydroxide. They suggested that this compound is precipitated at the ratio $[NaOH]_{excess}/[Fe(OH)_2] = 1$. This ratio is equivalent to the definition of X_b. The first oxidation reaction [III.21] at point A_1 becomes therefore:

$$Fe(OH)_2 + 1/4\ O_2 + 1/2\ H_2O \rightarrow Fe(OH)_3 \qquad \textbf{[III.23]}$$

Since all the iron atoms in this intermediate compound are obviously in the ferric state, one would expect it to be a possible stable end product of oxidation. Although both ASTM (III.80) and Van der Giesen (III.2) report a cubic $Fe(OH)_3$ structure, there is no clear evidence that any such stable crystalline $Fe(OH)_3$ exists; at least a part of such precipitates seems to be FeOOH (III.27; III.82-III.84). Thus, this colloidal gel, often found in iron rusts, could better be described in its partially dehydrated form as $FeO_m(OH)_{3-2m}$ or mFeOOH, (1-m)$Fe(OH)_3$ or FeOOH, (1-m)H_2O. Several others authors (III.69) obtained practically the same diffraction lines as the cubic structure but indexed in hexagonal lattices. It can, however, be accepted that this variety of small particle gel, with particle sizes of about 10-90 A (III.26; III.69; III.83; III.84), conserves the hexagonal stacking of the anions as they are in δ-FeOOH. They are also paramagnetic at room temperature and have the same color as δ-FeOOH. Under the conditions of their experiments, they relate it to possible undeveloped nuclei of geothite and it shall be labeled as inactive α'-FeOOH. This

subject is further discussed by them in a separate publication in their series (III.69). Their analysis is partially in agreement with the mechanism of Misawa et al. (III.57) for the formation of geothite in a strongly alkaline solution, along the line:

$$Fe(OH)_2 \xrightarrow{1} Fe(OH)_3^- \xrightarrow{2} Fe(OH)_{3aq} \xrightarrow{3} FeO_m(OH)_{3-2m} \xrightarrow{4} \alpha\text{-}FeOOH \qquad \text{[III.24]}$$

Point A_2. Recent investigation on δ-FeOOH and ferrihydrites (III.69) seems to show that the actual trigger value for point A_2 is R = 0.417 = 5/12 not far from the experimental value of 0.4 reported here.

The oxidation reaction at point A_2 would then be

$$5\ Fe(OH)_2 + 1/2\ O_2 + H_2O \rightarrow 3\ Fe(OH)_2,\ 2\ Fe(OH)_3 \qquad \text{[III.25]}$$

This intermediate compound will most likely be formed in the basic medium as it does not contain any other foreign anion apart from oxygen. It can easily be oxidized to the hexagonal crystal of δ-FeOOH, or any other possible hexagonal crystal.

The oxidation reaction of the intermediate compound would be

$$3\ Fe(OH)_2,\ 2\ Fe(OH)_3 + 3/4\ O_2 \rightarrow 3\ FeOOH,\ 2\ Fe(OH)_3 + 3/2\ H_2O \qquad \text{[III.26]}$$

The clear evidence that point A_2 is a characteristic point suggests that part of the paramagnetic component, observed by Mössbauer spectroscopy, could be the crystal 3 FeOOH, 2 $Fe(OH)_3$, usually given for ferrihydrite (III.85; III.86).

General Mechanism of Oxidation. From all analyses made above, the general mechanism of oxidation of ferrous hydroxide in the basic medium (i.e. for R < 0.5) is as follows:

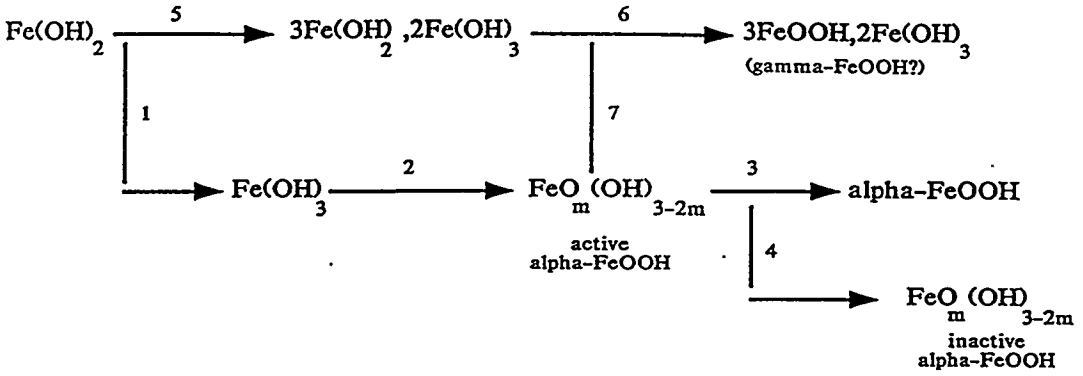

[III.27]

One would expect that in a strongly alkaline solution, path 1-2-3, which also partially represent the mechanism of Misawa, will be more favorable. Krause et al. (III.77) observed that the solubility of oxygen in water decreases with basicity. The decrease in the rate of oxidation with the increase in alkalinity, as seen from Fig. III.35, can be explained in terms of the production of OH^- ions from equation III.20.

Stoichiometric Condition (R = 0.5). From equation II.14, the transition point B corresponds to the value of R when $Fe(OH)_2$ can stoichiometrically be precipitated from the reacting chemicals. It has earlier (III.73; III.75; III.87; III.88) been shown that magnetite always dominates as the oxidation end product at this stoichiometric condition irrespective of the reacting medium. Several other authors (III.89-III.91) have observed that magnetite is preferentially formed at pH between 9 and 11; this can be seen from Figure III.34 to correspond to the value R = 0.5.

Agreement is yet to be reached on the mechanism of formation of magnetite from ferrous hydroxide. It is quite certain from the experiments described in the above experiments that neither the basic intermediate compound nor GR2 can be formed at point B. It is possible to obtain magnetite by direct oxidation of ferrous

hydroxide. This is quite reasonable since, at point B, the solution is free of excess Fe^{2+} and OH^- ions. Start by assuming arbitrary values m and p such that the anodic and cathodic reactions will respectively be:

$$\begin{array}{c} 3\ Fe(OH)_2 = Fe_3O_m(OH)_p + (6-m-p)H_2O + (2m+p-6) \\ 1/2\ O_2 + H_2O + 2e^- \rightarrow 2\ OH^- \end{array} \qquad \text{[III.28]}$$

The electrical neutrality of the solution requires that p = 8 - 2m. The global reactions are thus:

$$3\ Fe(OH)_2 + 1/2\ O_2 \rightarrow Fe_3O_m(OH)_{8-2m} + (m-1)H_2O \qquad \text{[III.29]}$$

$$Fe_3O_m(OH)_{8-2m} \rightarrow Fe_3O_4 + (4-m)H_2O \qquad \text{[III.30]}$$

It should be noted that by initially assuming these arbitrary values m and p, it turns out that we obtain an intermediate compound $Fe_3O_m(OH)_{8-2m}$ which has the same oxidation state as magnetite. Olowe and Genin consider this hypothesis acceptable under the conditions of their experiments.

This is similar to Hiller and Schwartz's mechanism (III.93, III.94) if the intermediate compound is considered to be two separate compounds and if m = 2:

$$Fe(OH)_2 + 2\ FeOOH = Fe_3O_4 + 2\ H_2O \qquad \text{[III.31]}$$

Girard and Chaudron (III.94), by inducing a reaction between ferrous hydroxide and α-Fe_2O_3, observed that magnetite is formed as the end product. Their proposed mechanism is as follows:

$$Fe + 2\ H_2O \rightarrow Fe(OH)_2 + H_2$$
$$Fe(OH)_2 + Fe_2O_3 \rightarrow Fe_3O_4 + H_2O \qquad \text{[III.32]}$$

They suggested that the reaction passes through a green intermediate compound with the same oxidation state as magnetite, and thus described it as hydrated magnetite with a chemical formula Fe_3O_4, nH_2O. Olowe and Génin consider that it is certain that this intermediate compound is neither GR2 nor similar to the basic compound as they believed. Nevertheless, their (III.94) last equation is also similar to equation [III.30] by putting m = 3.

Bernal et al. (III.51) also suggested that, in a neutral solution, $Fe(OH)_2$ is in equilibrium with a ferrous-ferric compound $Fe_3(OH)_8$ which transforms to magnetite. Olowe and Génin note that this ferrous-ferric compound is equivalent to our intermediate compound ($Fe_3O_m(OH)_{8-2m}$) by putting m = 0.

Misawa et al. (III.58) observed that magnetite can be formed by the neutralization and dehydration of a 'dark red complex (DRC)' which is precipitated in acid solutions (pH < 5). They observed that DRC has the same Fe^{2+}:Fe^{3+} ratio as in magnetite, and that the latter is not formed until the pH rises to about 7.2. They proposed that magnetite is formed from DRC as follows:

$$[Fe(II)_1Fe(III)_2O_x(OH)_{2(3-x)}]_m^{2m+} + 2mOH^- = mFe_3O_4 + (4-x)H_2O \qquad \text{[III.33]}$$

Olowe and Génin therefore concluded, from all indications, that magnetite is always formed from an intermediate which contains the same Fe^{2+}:Fe^{3+} ratio. This justified their hypothesis since the initial product is the solid phase, ferrous hydroxide.

If one compares the Fe/O ratio (1/2) in ferrous hydroxide, which also corresponds to the value of R at point B, with that in the proposed intermediate $Fe_3O_m(OH)_{8-2m}$, the value of m will most likely be equal to 2.

Hence at point B, the mechanism of oxidation of pure ferrous hydroxide is:

$$3\ Fe(OH)_2 + 1/2\ O_2 \rightarrow Fe(OH)_2,\ 2FeOOH + H_2O$$
$$Fe(OH)_2,\ 2FeOOH \rightarrow Fe_3O_4 + 2\ H_2O \qquad \text{[III.34]}$$

Acidic Medium (R > 0.5). One should recall from equations [III.17] and [III.18] that X_a is the concentration ratio of the excess Fe^{2+} or SO_4^{2-} ions to that of the precipitated $Fe(OH)_2$. For the two characteristic values C and D one has:

for C (R = 4/7) $X_a = 1/7$;

for D (R = 7/12) $X_a = 1/6$.

Point C. At point C, all excess SO_4^{2-} ions will be consumed to completely oxidize the initial ferrous hydroxide (FH) into Green Rust 2 (GR2), and thus leaving the excess Fe^{2+} ions in the solution. It is well known (III.2; III.82; III.95-III.98) that the formation of geothite is favored by the presence of Fe^{2+} or OH^- ions in the solution. However, point C from the experiments of Olowe and Génin is a characteristic point where geothite dominates as the end product. The reactions at point C can be presented as follows (the general formula adopted for GR2 will be supported later):

$$8\ FeSO_4 + 14\ NaOH \rightarrow 7\ Fe(OH)_2 + 7\ Na_2SO_4 + Fe^{2+} + SO_4^{2-} \qquad \text{[III.35]}$$

globally,

$$7\ Fe(OH)_2 + Fe^{2+} + SO_4^{2-} = Fe_7O_{2m}(OH)_{14-4m}SO_4 + 2mH_2O + Fe^{2+} + 2e^- \quad [III.36]$$
$$1/2\ O_2 + H_2O + 2e^- = 2\ OH^-$$

$$7\ Fe(OH)_2 + Fe^{2+} + SO_4^{2+} + 1/2\ O_2 \rightarrow GR2 + (2m-1)H_2O + Fe^{2+} + 2OH^- \quad [III.37]$$

where GR2 is $Fe_7O_{2m}(OH)_{14-4m}SO_4$.

From equation [III.37], the formation of GR2 is accompanied by an enrichment of the solution in OH^- and hence a rise in pH as observed on the pH curves (point noted TE in Figure III.33). The formation of geothite in the presence of Fe^{2+} ions is still far from being well understood. Schindler et al. (III.82) and François et al. (III.96) simply put it that the effect of Fe^{2+} is catalytic. Olowe and Génin simply write the formation of geothite from GR2 as follows:

$$Fe_7O_{2m}(OH)_{14-4m}SO_4 \xrightarrow{Fe^{2+}OH^-} \alpha-FeOOH \quad [III.38]$$

Point D. The formation of GR2 at point D from ferrous hydroxide (FH) is as follows:

$$7\ FeSO_4 + 12\ NaOH \rightarrow 6\ Fe(OH)_2 + 6\ Na_2SO_4 + Fe^{2+} + SO_4^{2-} \quad [III.39]$$

$$6\ Fe(OH)_2 + Fe^{2+} + SO_4^{2-} = Fe_7O_{2m}(OH)_{14-4m}SO_4 + (2m-2)H_2O + 2H^+ + 2e^- \quad [III.40]$$
$$1/2\ O_2 + H_2O + 2e^- = 2\ OH^-$$

and combined,

$$6\ Fe(OH)_2 + Fe^{2+} + SO_4^{2+} + 1/2\ O_2 \rightarrow GR2 + (2m-1)H_2O \qquad \textbf{[III.41]}$$

It can be seen that the only difference between [III.37] and [III.41] is that, in the latter, the solution is deprived of both the excess Fe^{2+} and SO_4^{2-} ions in the course of formation of GR2. It is well known (III.53; III.74; III.95; III.97; III.98) that lepidocrocite is a by-product of green rust compounds. This is compatible with the observation at point D (where lepidocrocite suddenly appears at its maximum) as the solution will practically be free of Fe^{2+} ions if reaction [III.40] is followed. It can therefore be implied that lepidocrocite is obtained here by direct oxidation of 'pure' GR2. Its mechanism of formation would likely be as follows:

$$Fe_7O_{2m}(OH)_{14-4m}SO_4 + O_2 \rightarrow 6(\gamma\text{-}FeOOH) + (4-2m)H_2O + FeSO_4 \qquad \textbf{[III.42]}$$

Between points D and E, GR2 will be formed as in equation [III.41], but the extra $FeSO_4$ added into the solution will favor the formation of geothite, and hence the proportion of lepidocrocite will continuously diminish. Point E corresponds to the beginning of formation of sulphated ferrous hydroxide (SFH) as described by equation [III.18].

The Chemical Formula of GR2. It can be seen that the behavior of the pH curves and the results of Mössbauer analysis are explainable from the proposed general formula of GR2. No matter what other arguments one can use to explain

these behaviors and simultaneously be compatible with practical observations, one will arrive at the conclusion that GR2 is:

$$Fe_7O_{2m}(OH)_{14-4m}SO_4,nH_2O$$

or

$$4Fe(OH)_2,2FeO_m(OH)_{3-2m},FeSO_4,nH_2O$$

The Mössbauer effect evidence of a ferrous sulphate layer in the crystal structure of GR2 (III.101), shows that its chemical formula is better written as in the second case. The value m/2 represents (as in the basic medium) the extent of deprotonation of the initial hydroxide.

Feitknecht and Keller (III.100), in their early work, obtained a green compound with about 238% of Fe^{3+} ions in the sulphate medium. This corresponds within experimental accuracy to the proportion (28.57% = 2/7) of Fe^{3+} ions in GR2.

The given general formula is an exact of that given by Derie et al. (III.97; III.98) by taking m to be 0, i.e. $4Fe(OH)_2$, $2Fe(OH)_3$, $FeSO_4$, nH_2O. They obtained the value 2.5 for the ratio Fe^{2+}:Fe^{3+} in GR2. All their other analyses (III.103) supported their formula. Gancedo et al. (III.102), from Mössbauer investigation, also obtained the value 2.63 for the Fe^{2+}:Fe^{3+} ratio in GR2, and hence supported the Derie et al. formula.

If the argument of Misawa et al. (III.58) that GR2 must contain both hydroxo- and oxo- bridges is accepted, as it is an intermediate compound between ferrous hydroxide and the oxyhydroxides, then m will not likely be 0.

Tamaura et al. (III.103), by chemical analysis, obtained the value 2 for the Fe^{2+}:Fe^{3+} ratio; they gave the general formula of GR2 as $Fe_3^{2+}Fe_1^{3+}(OH)_{5-2m}O_mSO_4$. This formula contains too much of SO_4^{2-} ions to be able to explain all observations made so far. However, from their last analysis (III.54) in an effort to form GR2 by the insertion of γ-FeOOH into $Fe(OH)_2$, $2FeO_m(OH)_{3-2m}$, $FeSO_4$, nH_2O, can take three values to arrive at the three possible chemical formulate for GR2:

$$\left.\begin{array}{lll} (i) & 4Fe(OH)_3, 2Fe(OH)_3, FeSO_4, nH_2O & (for\ m=0) \\ (ii) & 4Fe(OH)_2, FeOOH, Fe(OH)_3, FeSO_4, nH_2O & (for\ m=1/2) \\ (iii) & 4Fe(OH)_2, 2FeOOH, FeSO_4, nH_2O & (for\ m=1) \end{array}\right\} \quad \text{[III.43]}$$

The most likely chemical formula would be that given by (iii) if we compare the Fe/O ratio in the compound, leaving out the oxygen from $FeSO_4$, nH_2O which is not affected by deprotonation, to the value of R = 7/12 at point D where the formation of GR2 can be considered to be a result of direct oxidation of ferrous hydroxide (equation [III.41]) rather than at point C (equation [III.37]).

Geothite is the most dominant of the end products (especially at very high and low values of R) but it paves way, almost totally for magnetite and lepidocrocite at points B and D respectively, and partially for another crystalline product (probably δ-FeOOH) at point A_2. These characteristic points correspond to compositions where

direct oxidation of intermediate compounds take place. Geothite thus needs some excess Fe^{2+} or OH^- ions for its formation.

The identity of oxidation compounds of iron at the different characteristic values of R are given in Table III.6.

Table III.6

Identified Intermediate Compounds During the Oxidation of Ferrous Hydroxide in the Presence of SO_4^{2-} Ions at Different Characteristic Values of R. The Given Values of x Correspond to the Stoichiometric Coefficients of the Initial Ferrous Hydroxide Involved in the Transformations

	R	Intermediate (name)	x	End Product (name)
A_1	1/3	$FeO_m(OH)_{3-2m}$ (amorphous active α-FeOOH)	1	α-FeOOH (geothite)
A_2	5/12	$3Fe(OH)_2,2Fe(OH)_3$ (basic compound)	5	$3FeOOH,2Fe(OH)_3$ (δ-FeOOH ?)
B	1/2	$Fe(OH)_2,2FeOOH$ (hydrated magnetite)	3	Fe_3O_4 (magnetite)
C	4/7	$4Fe(OH)_2,2FeOOH,FeSO_4,nH_2O$ (green rust two)	7	α-FeOOH (geothite)
D	7/12	$4Fe(OH)_2,2FeOOH,FeSO_4,nH_2O$ (green rust two)	6	γ-FeOOH (lepidocrocite)
E	5/8	$4Fe(OH)_2,FeSO_4,nH_2O$ (sulphated ferrous hydroxide)*	4	α- and γ-FeOOH

* Sulphated ferrous hydroxide is an initial product; the intermediate product at this value of R is still green rust 2.

III.G. Precipitations with Seeding

This subject offers a fruitful area of research. It is reasonable to assume that industrial recipies contain steps that may employ seeding; however, references to this in the open literature is very sparse.

In many precipitations the situation is complicated by the presence of two or more solid-growing phases. Van der Woude, et al. (III.12) made an analysis of the relaxation curves by means of Eq. [III.12] is complicated by the presence of two different growing phases (amorphous and crystalline hematite) in most of the experiments in studies in reference (III.12). To get more information about the growth mechanism of hematite, they performed a number of seed experiments. One might expect the presence of excess hematite particles to suppress the formation and growth of the amorphous phase. In addition, the relaxation may be assumed to occur at approximately constant total surface, depending on the total amount of added seed material. Growth curves at constant pH were measured over the same α_o range as was involved in the relaxation studies in the absence of seed. Examples of these growth curves are given in Figure III.39. Conspicuous is the absence of S-shaped curves. The total reaction time is also considerably shortened in comparison with unseeded growth. In all the seed experiments, except for that one with $\alpha_o = 0.20$, the supernatant was noted to be clear and colorless after conclusion of the relaxation. This observation points to the absence of the amorphous phase in most of these experiments.